

Electronic Supplementary Information

Unravelling the Modus-Operandi of Chromenylium-Cyanine Fluorescent Probes: A Case Study

Ricardo Flores-Cruz, ^a *Rafael López-Arteaga,* ^a *Lizbeth Ramírez-Vidal,* ^b *Fernando López-Casillas* ^b and *Arturo Jiménez-Sánchez* ^{a*}

^a Instituto de Química, Universidad Nacional Autónoma de México, México D.F. No. 04510, México. * arturo.jimenez@iquimica.unam.mx

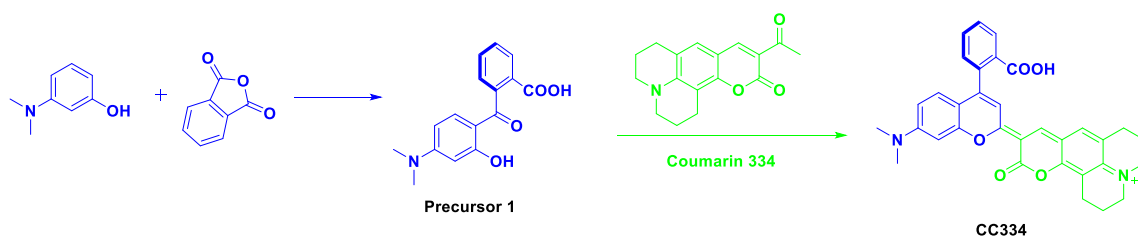
^b Instituto de Fisiología Celular, Universidad Nacional Autónoma de México, México D.F. No. 04510, México.

METHODS

General Probe Synthesis

Starting materials and solvents were commercially available and used without further purification. Compound **CC334** was synthesized according to a previously reported procedure.¹ Specifically, a solution of 3-(dimethylamino)phenol (2.00 g, 15 mmol, Sigma-Aldrich, Mexico) and phthalic anhydride (2.60 g, 18 mmol, Sigma-Aldrich, Mexico) were refluxed in toluene for 24 hours, then the solvent was removed by evaporation at reduced pressure and 100 mL of 35% NaOH aq solution was added and further stirred for 12 hours. Then, after acidification with 1M HCl the precipitate was filtered and recrystallized from MeOH : H₂O obtaining 3.60 g of a pale brown crystalline powder of precursor **1** (85% yield). Then, precursor **1** (417 mg, 1.48 mmol) was immediately added to solution of coumarin 334 (500 mg, 1.75 mmol) in 8mL H₂SO₄ at 0°C and stirred at 90°C for 12 hours. Then after reaching room temperature, 5 grams of ice were added to the crude product following with 800 µL HClO₄ addition. The crude product precipitated and was filtered, extracted (dichloromethane : brine, 4X) and dried under anhydrous Na₂SO₄. Then, the product was purified by RP-HPLC using an isocratic method, with a mixture of MeOH : H₂O (70:30 v/v)

as eluent. The column was a Luna 5u C18 (2) 100 Å, 50 x 21 mm, 5 microns. A flow of 10 mL/min was used and 500 µL of **CC334** solution was injected (50 mg/2 mL of MeOH). The main impurity comes out at 5 min and ends at 10 min while **CC334** has a retention time of 15 min. The product was recovered, and the solvents were evaporated. *Right:* is shown a representative RP-HPLC chromatogram. A dark-green powder was obtained (149 mg, 20% yield). ¹H NMR (700 MHz, MeCD₃) δ/ppm 8.51 (s, 1H), 8.09 (s, 1H), 7.88 (s, 1H), 7.61 (dt, *J* = 7.7 Hz, 2H), 7.31 (s, 1H), 7.18 (s, 1H), 6.88 – 6.73 (m, 3H), 3.42 (m, 4H), 3.05 (s, 6H), 2.67 (m, 2H), 2.45 (m, 2H), 1.93 (m, 4H). ¹³C{¹H} NMR (175 MHz, MeCD₃) δ/ppm 171.5, 161.6, 161.2, 157.8, 156.8, 155.4, 152.1, 150.4, 144.2, 134.3, 129.1, 128.9, 128.7, 128.5, 128.2, 128.1, 127.9, 120.8, 114.5, 114.4, 111.3, 109.6, 104.7, 102.7, 95.9, 49.8, 49.3, 38.8, 28.7, 26.0, 19.7, 18.7, 18.6. UV-Vis in methanol λ/nm (ε/dm³ mol⁻¹ cm⁻¹) 650 (180760). The measured fluorescence quantum yield of **CC334** in methanol was 0.063 using coumarin 343 as standard. ESI HRMS-TOF: *m/z* 533.2077 [M-H]⁺ found, 533.21 calculated.



Scheme S1. Synthetic methodology for probe **CC334**.

Preparation of ROS agents:

- 1) Hydrogen peroxide (H₂O₂), Sodium hypochlorite (NaClO), Iron(III) chloride (FeCl₃), Sodium bicarbonate (NaCO₃), Sodium nitrate (NaNO₃) and Sodium nitrite (NaNO₂) were obtained from Sigma-Aldrich and used as provided. Sodium peroxyxynitrite (NaNOO₂) was purchased from Merck Millipore (US1516620-1SET) and used as provided.
- 2) Singlet oxygen (¹O₂) was prepared as follows: The singlet oxygen concentration was determined by the following reaction: NaClO + H₂O₂ → NaCl + ¹O₂ + H₂O. The following was mixed: NaClO = [14%] (1 mL) with H₂O₂ = [30%] (2 mL) where the limiting reagent is sodium hypochlorite. So, 1mL NaClO (14%) is equiv. to 0.14 g of pure NaClO, giving 0.6266 M of NaClO. Then, a dilution was made 1 mL in 40 mL to obtain a 1.6 µM NaClO solution. After that a linear regression analysis was performed using the commercially available Singlet Oxygen Sensor Green®, as described in literature (Singlet Oxygen Production in Water: Aggregation and Charge-Transfer Effects. The Journal of Physical Chemistry, 1996, 100(16), 6555–6560).
- 3) Superoxide ion (O₂^{•-}): was prepared by reaction of commercially available potassium dioxide (KO₂, Sigma-Aldrich, 278904) and DMSO using supporting electrolyte and

tetrabutylammonium, as previously reported [M. Hayyan, M. A. Hashim, I. M. AlNashef, *Chem. Rev.* 2016, **116**, 3029–3085.].

Hydroxyl radical (OH[•]) were produced by Fenton reaction using 10 equiv. H₂O₂ + 1 equiv. FeCl₂.

Computational methodology.

Molecular geometry optimizations were obtained by Density Functional Theory (DFT) as performed in the Gaussian 09 code.² The intramolecular charge transfer (ICT) properties of **CC334** were first analyzed by using TD-DFT with polarizable continuum model by using the integral equation formalism (for water).^{3,4} Hybrid functionals such as PBE0 have been found to be very accurate for CT parameters and excited states in charge transfer molecular systems.⁵ Then, we used the PBE0/6-31+G(d)/IEF-PCM level of theory. Single electronic excitation by Natural Transition Orbital (NTO) analysis were carried out at the same level of theory.

Steady State Spectroscopy.

Absorption spectra were acquired in a 10 mm path-length quartz-cell Cary-50 (Varian) spectrophotometer, the emission and excitation spectra, in a Cary Eclipse (Varian) fluorimeter at room temperature (20 ± 1 °C) under aerated conditions.

Time-Correlated Single-Photon Counting.

The Time-Correlated Single-Photon Counting system has been previously described.⁶⁻⁸ Briefly, a 405 nm picosecond laser (LDH-D-C-405, PicoQuant) was coupled to a custom-built confocal microscope where the same 10 mm quartz-cell was placed. The collected fluorescence emission was separated from the excitation line with a 510 nm long-pass dichroic mirror (Chroma T510lpxrxt) and passed through a Notch filter (Chroma, ZET405nf) a BG40 filter (Newport) or a 655 nm long-pass (Chroma ET655LP), depending the emission band to detect. The fluorescence was focused to an avalanche photodiode (PD-050-CTE, Micro Photon Devices) synchronized to the laser controller (PDL 800-D) *via* a PicoHarp 300 module. The data was analyzed with SymphoTime 64 software.

Ultrafast Time-Resolved Emission.

The up-conversion setup has been described previously.⁹ One regeneratively amplified kHz of Ti:sapphire laser centered at 800 nm (1 mJ/pulse) of 80 fs in duration was split in two. The second harmonic of the fundamental pulse (400 nm, modulated at 1/3 of the laser repetition rate and magic-angle polarization) was generated in a 0.5 mm β-BBO crystal and excited the sample in a 1 mm flow cell. The fluorescence was collected with a pair of parabolic mirrors and refocused to the up-conversion β-BBO crystal where it was crossed with delayed-controlled ~1 mW of the 800 nm fundamental beam. The sum frequency signal was focused with a CaF₂ lens into a double 10 cm monochromator (Oriel) and detected with a photomultiplier tube. The up-conversion signal was digitalized with a lock-in amplifier (Stanford Research Systems). The instrument response function for the up-conversion experiments were determined to be Gaussian with a full width at half-maximum of 300 fs.

Optical microscopy.

HeLa cells were seeded in 8 well μ -slides (iBidi, Germany) at a density of 20000 cells per well one day prior to experiments in MEM alpha with 10% FBS. On treatment day, cells were washed once in MEM alpha with no FBS and incubated with 10 μ M probe **CC334** for 30 minutes. For experiments with TMRM, 10 nM TMRM (Thermo Fisher Scientific) was added 10 minutes before **CC334**. Cells were then washed twice in MEM alpha with no FBS and imaged using an inverted Zeiss LSM 880 microscope maintaining 5% CO₂ and 37°C during the experiments. On treatment day for fluorescence time course experiments, cells were incubated with 7 μ M probe **CC334** for 30 minutes in MEM alpha with 5% FBS for the indicated time at 37°C with 5% CO₂, then imaged at the same conditions.

Zebrafish lines and maintenance.

The experiments and handling of zebrafish were approved by the Committee for Laboratory Animal of the Universidad Nacional Autonoma de Mexico (UNAM), under the CICUAL-Protocol number: FLC40- 14. (CICUAL: “Comité Institucional para el Cuidado y Uso de los Animales de Laboratorio del Instituto de Fisiología Celular, Universidad Nacional Autonoma de Mexico”).

Zebrafish from AB strain were maintained in aquatic habitats recirculation system at 28°C with a dark/light period 14-10hr respectively. Embryos were obtained from natural mating, all the embryonic stages were determined according to (Kimmel et al. 1995). All embryos were treated with 0.2 mM 1-phenyl-2-thio-urea (Sigma Aldrich) to prevent pigmentation and permit posterior imaging.

Zebrafish imaging.

Embryos were stained with **CC334** for 30minutes, 4 hours or overnight with the indicated concentrations of the compound, embryos were washed in zebrafish water 3 times for 5-10minutes. All embryos were anesthetized with tricaine 4.2% (Sigma), some embryos were stimulated with ¹O₂ for 1 or 2 minutes at the indicated concentrations. Immediately the embryos mounted in 1% low melting point agarose (National Diagnostics), images were acquired from living zebrafish embryos with stereomicroscope Nikon SMZ1500 or confocal microscope Zeiss LSM800.¹⁰

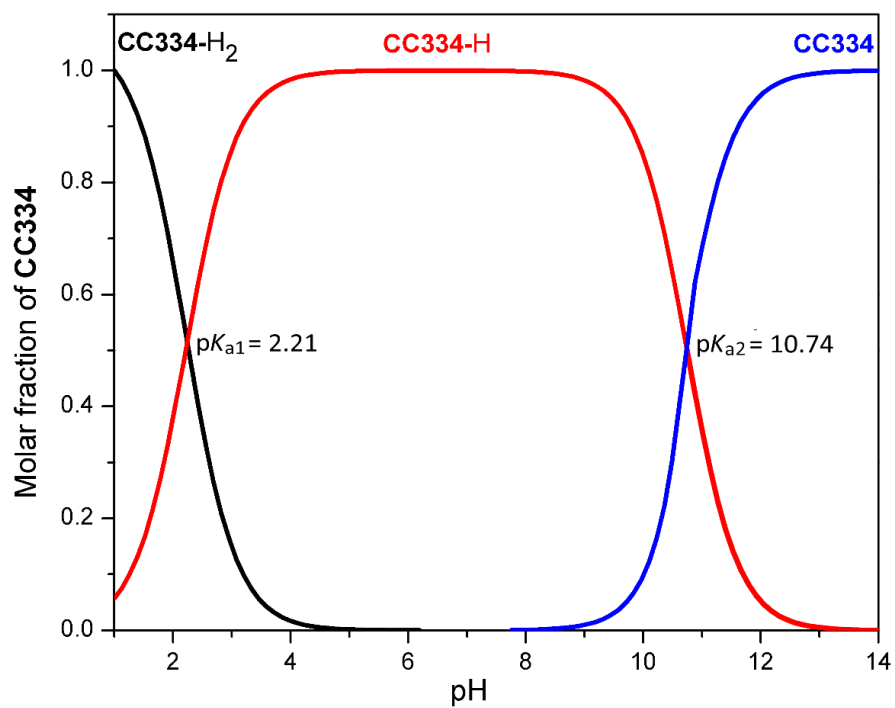


Fig. S1. Concentration distribution curves of **CC334** (5 mM) in 50 mM NaCl at 25 °C. The molar fractions are plotted using potentiometric constants. **CC334-H₂** (dicationic), **CC334-H** (monocationic), **CC334** (neutral-closed form).

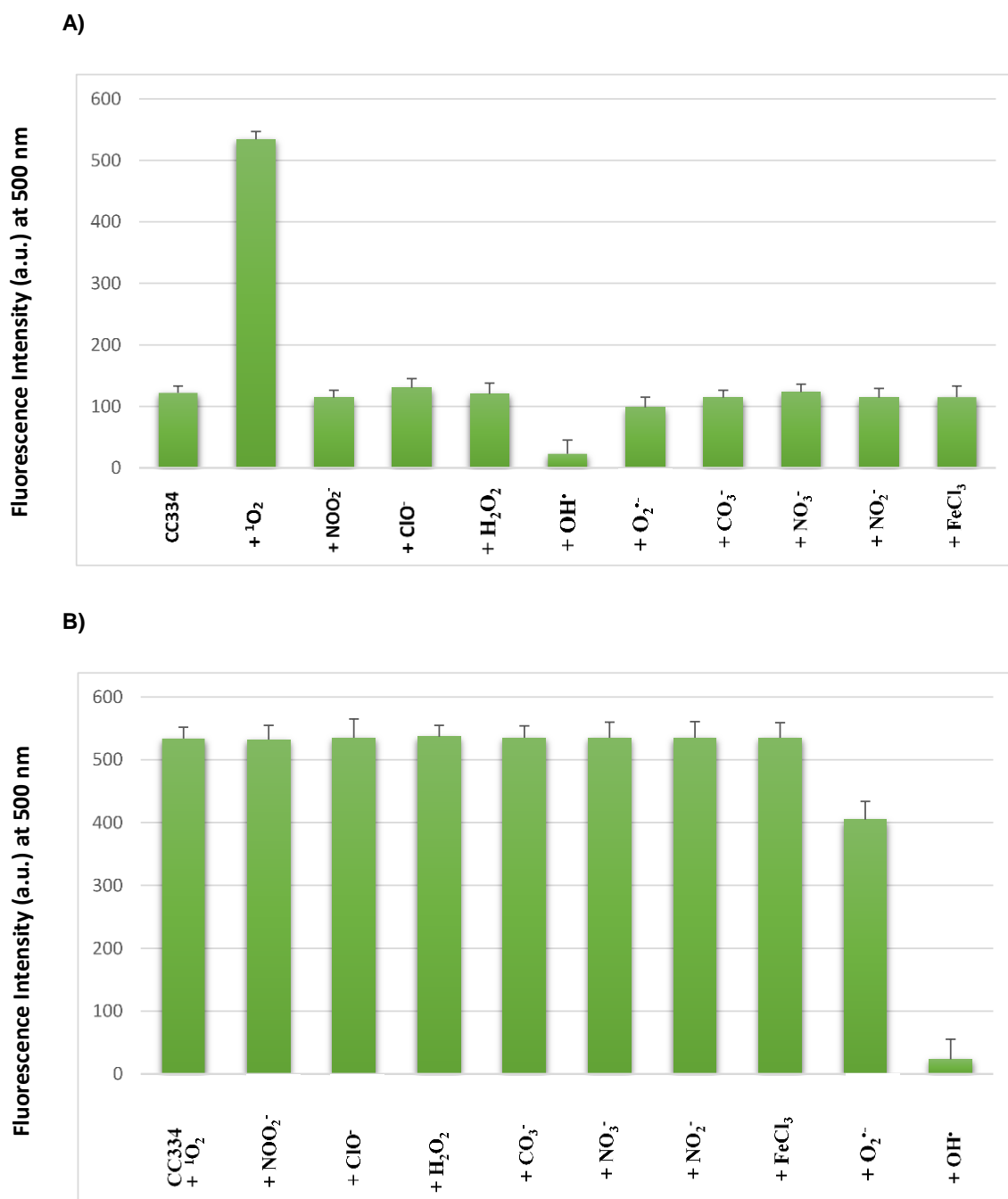
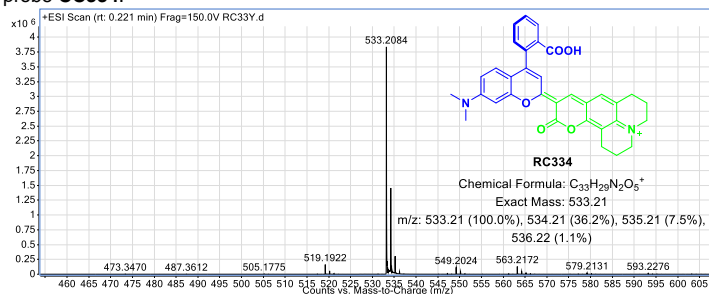
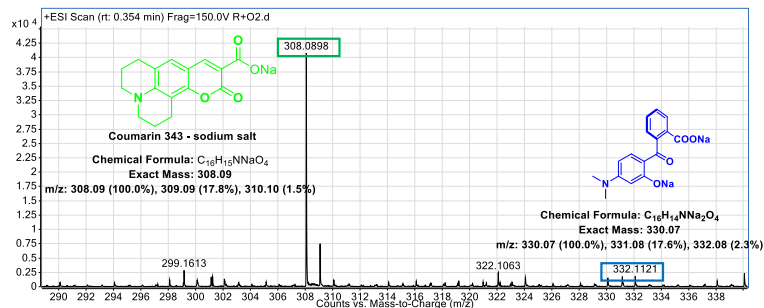


Fig. S2. Selectivity and competition graphs. A) Fluorescence intensity bars at $\lambda_{\text{em}} = 500 \text{ nm}$ for **CC334** under different oxidants. B) Competition experiments for **CC334**+ $^1\text{O}_2$ with different oxidants. NOO_2^- = Peroxynitrite, ClO^- = Hypochlorite, H_2O_2 = Hydrogen peroxide, CO_3^- = Bicarbonate, NO_3^- = nitrate, NO_2^- = nitrite, FeCl_3 = Ferric chloride, $\text{O}_2^{\cdot-}$ = Superoxide, OH^\cdot = Hydroxyl radical. All ROS species concentrations are in 1000% molar excess (0.8 M) with respect to the **CC334**.

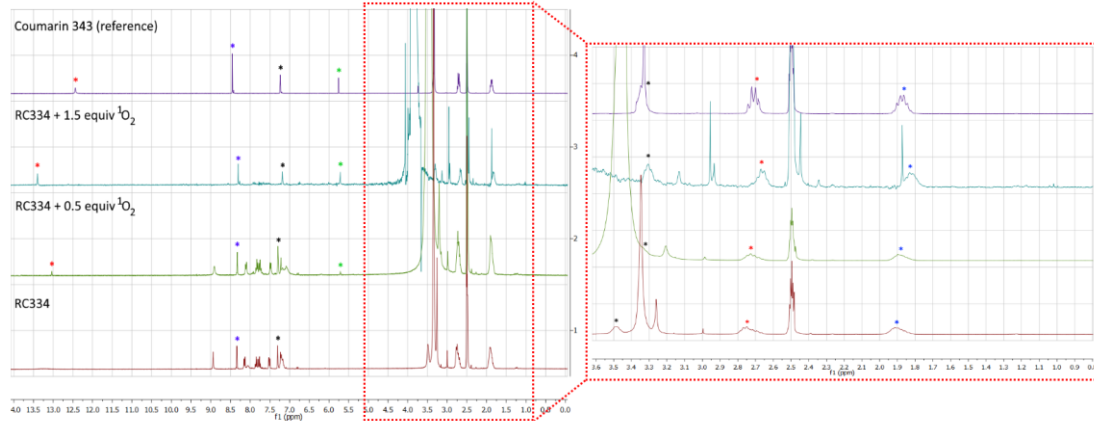
A) ESI-TOF scan for probe **CC334**.



B) ESI-TOF⁺ scan for probe **CC334** after 1 equivalent addition of singlet oxygen.



C) ¹H-NMR spectra for the ¹O₂ titration of probe **CC334**. Coumarin 343 spectrum is show as reference control.



D)

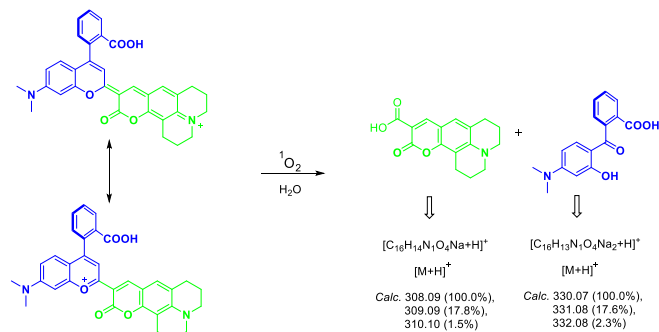


Fig. S3. A) and B) High-Resolution Mass Spectrometry (ESI-TOF technique) and, C) ¹H-NMR titrations for **CC334** with ¹O₂. D) Schematic representation for the oxidation mechanism.

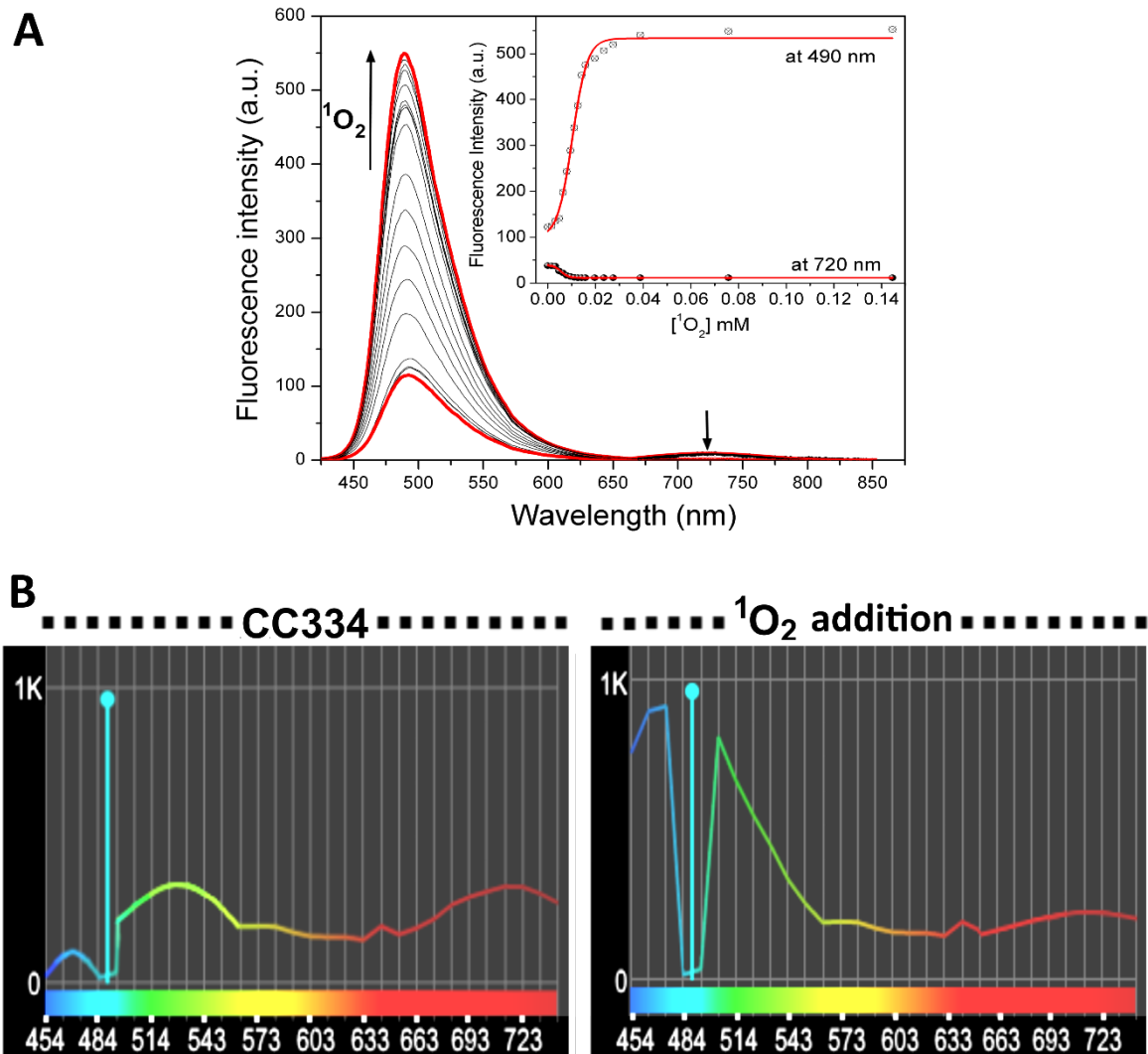


Fig. S4. Differential mitochondria-nucleoli re-localization dynamic of **CC334**. Panel A shows the **CC334** titration with $^1\text{O}_2$. Panel B shows the real-time fluorescence profile of **CC334** spectrally-resolved upon interaction with $^1\text{O}_2$.

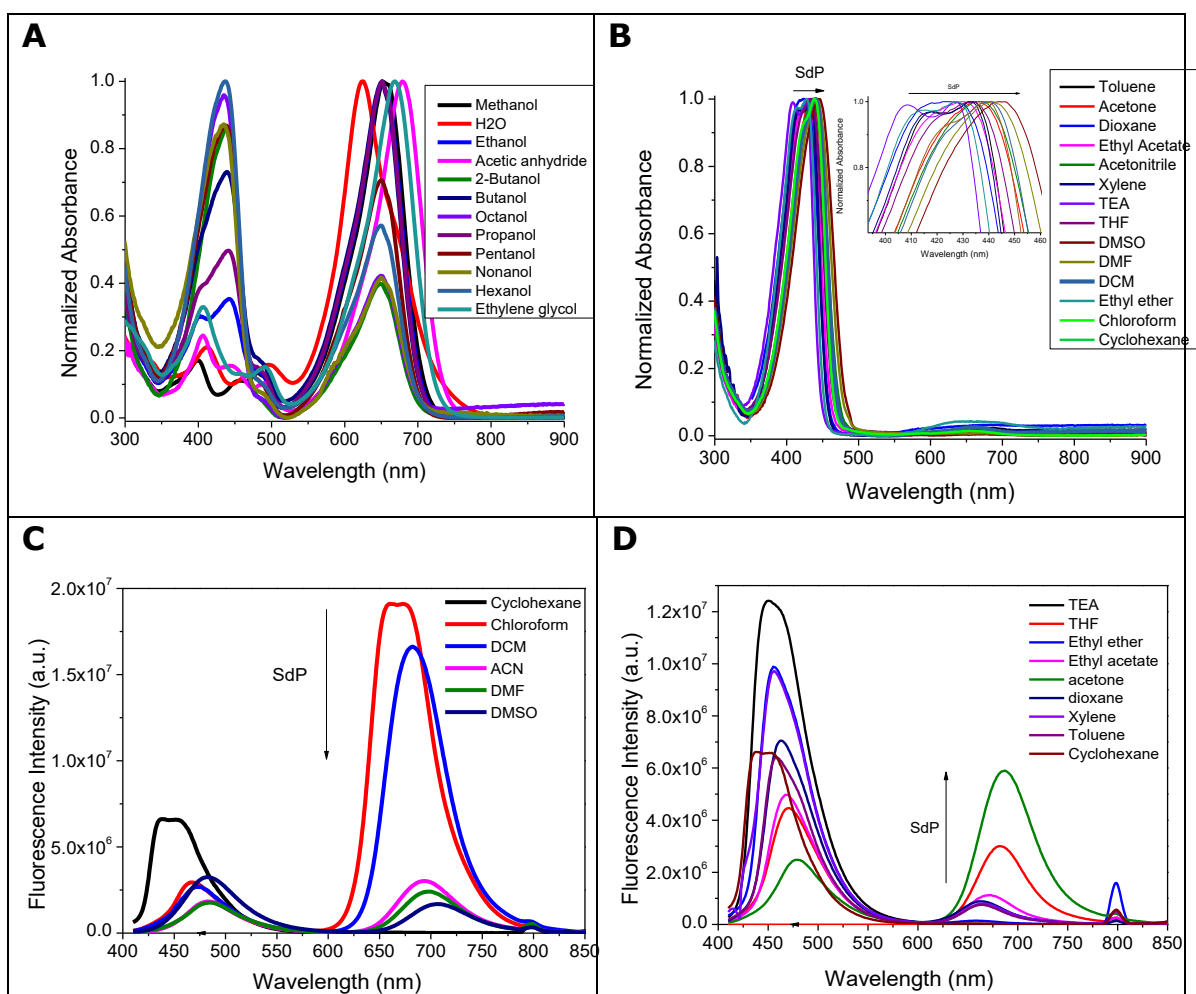


Fig. S5. Absorption spectra of CC334 in different protic (A) and non-protic (B) solvents, respectively. (C) and (D) show the fluorescence spectra in different solvents, SdP indicates the solvent dipolarity influence.

Table S1A. Fitting parameters for the TCSPC histograms of the blue emission band of **CC334** in different solvents excited at 405 nm.

Eqs.	a ₁	τ ₁ [ns]	a ₂	τ ₂ [ns]	a ₃	τ ₃ [ns]	< τ >
Acetone	<1	3.7±0.	>99	<0.1	<1	0.6±0.	0.2±0.1
Acetonitrile	<1	3.8±0.	>99	<0.1	<1	0.6±0.	<0.1
Water	54	4.3±0.	46	0.9±0			3.8±0.1
Methanol	33	3.8±0.	67	0.5±0			3.2±0.1
Cyclohexane	17	2.9±0.	83	0.2±0			2.3±0.1

Table S1B. Fitting parameters for the TCSPC histograms of the red emission band of **CC334** in different solvents excited at 405 nm.

Eqs.	a ₁	τ ₁ [ns]	a ₂	τ ₂ [ns]	< τ >
Acetone	100	0.7±0.			0.7±0.1
Acetonitrile	100	0.5±0.			0.5±0.1
Water	>99	<0.1	<1	2.9±0	0.6±0.1
Methanol	100	0.3±0.			0.3±0.1

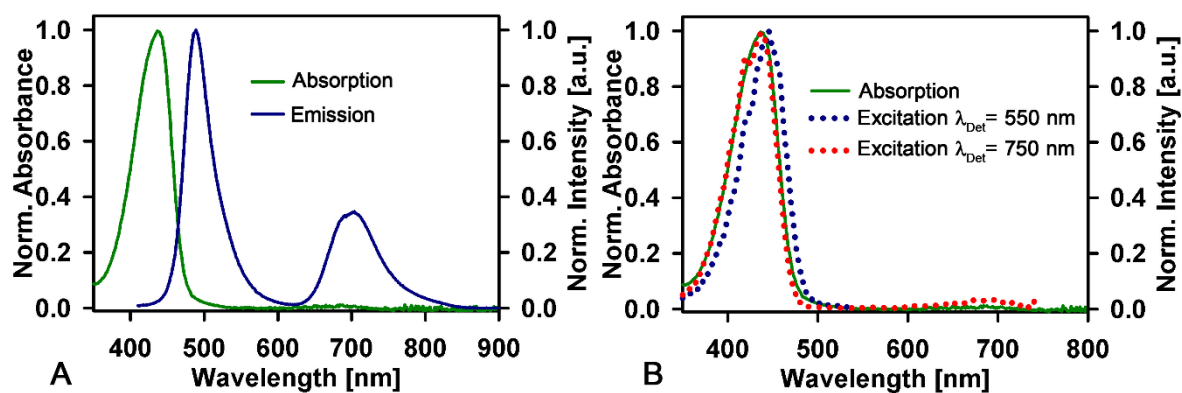


Fig. S6. A) Absorption and emission spectra of the probe **CC334** in acetone. B) Absorption and excitation spectra of the probe **CC334** in acetone, detecting the blue and red emission bands.

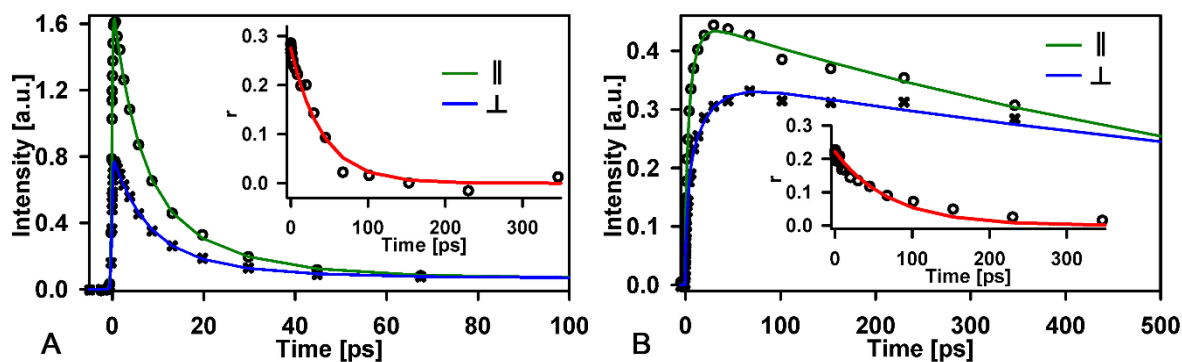


Fig. S7. Parallel and perpendicular fluorescence transients of the **CC334** probe in acetone, pumped at 400 nm and detected at A)520 nm and B)700 nm, the insets show their respective anisotropy decay.

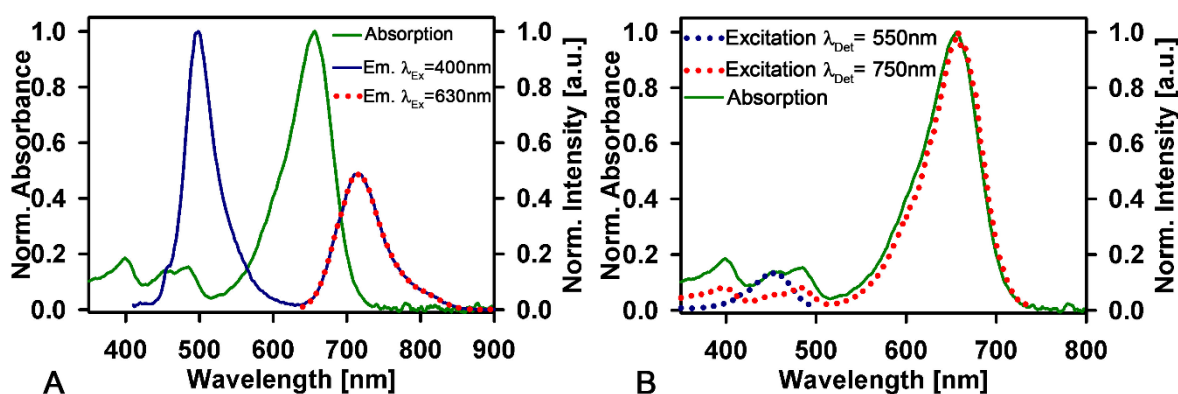


Fig. S8. A) Absorption and emission spectra of the probe **CC334** in methanol, exciting at both bands. B) Absorption and excitation spectra of the probe **CC334** in methanol, detecting the blue and red emission bands.

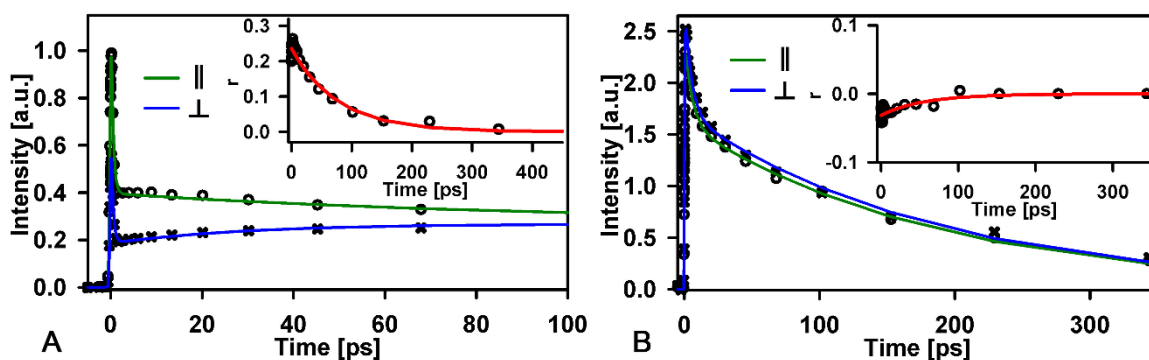


Fig. S9. Parallel and perpendicular fluorescence transients of the **CC334** probe in methanol, pumped at 400 nm and detected at A)520 nm and B)700 nm, the insets show their respective anisotropy decay.

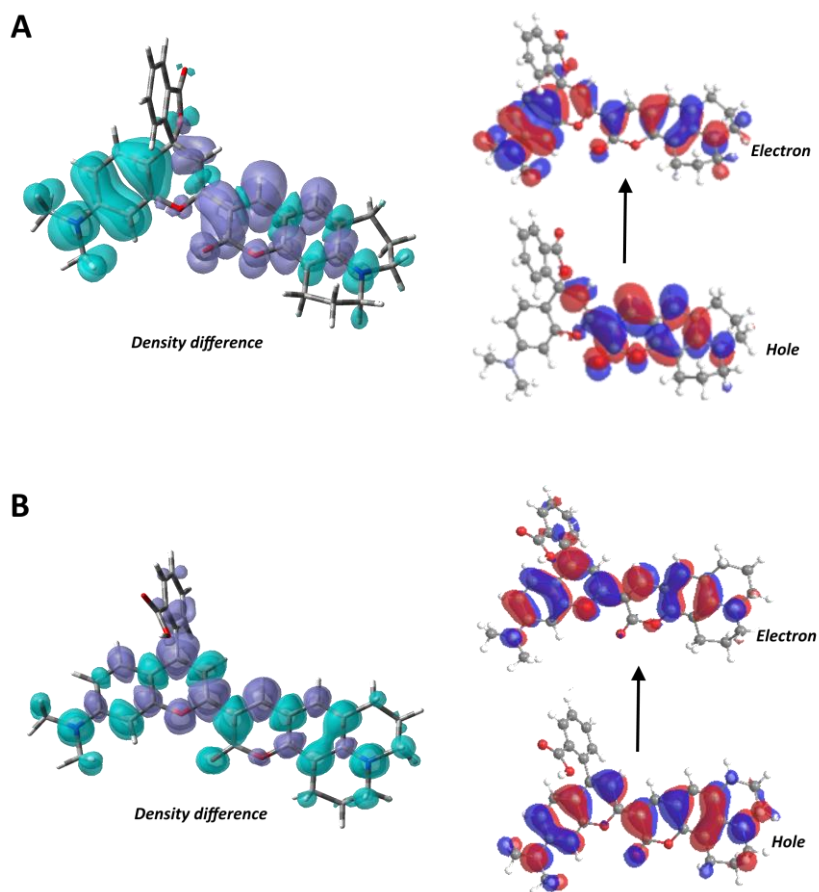


Fig. S10. a) Electron density differences between electronic ground and first excited state for **CC334** computed at PBE0/6-31+G(d,p)/IEF-PCM-Water (positive and negative variations of density are represented in purple and turquoise blue, respectively); and the corresponding b) HOMO and c) LUMO energy levels.

References

- [1] R. Flores-Cruz, A. Jiménez-Sánchez, *Chem. Commun.*, 2018, **54**, 13997-14000.
- [2] M. J. Frisch, et al. Gaussian 09, Revision C.02, Gaussian, Inc.: Wallingford CT, 2009.
- [3] C. Amovilli, V. Barone, R. Cammi, E. Cancès, M. Cossi, B. Mennucci, C. S. Pomelli, J. Tomasi, *Adv. Quantum Chem.*, 1998, **32**, 227–261.
- [4] J. Tomasi, B. Mennucci, R. Cammi, *Chem. Rev.*, 2005, **105**, 2999–3094.
- [5] C. Adamo, V. Barone, *J. Chem. Phys.*, 1999, **110**, 6158–6170.
- [6] R. López-Arteaga, J. Peón, *J. Phys. Chem. C*, 2018, **122**, 26698–26706.
- [7] L. Gutiérrez-Arzaluz, R. López-Arteaga, F. Cortés-Guzmán, J. Peón, *J. Phys. Chem. B*, 2017, **121**, 9910–9919.

- [8] J. Rodríguez-Romero, C. Guarín, A. Arroyo-Pieck, L. Gutiérrez-Arzaluz, R. López-Arteaga, F. Cortés-Guzmán, P. Navarro, P. Peon, *ChemPhotoChem*, 2017, **1**, 397–407.
- [9] J. S. Zugazagoitia, M. Maya, C. Damián-Zea, P. Navarro, H. I. Beltrán, *J. Phys. Chem. A*, 2010, **114**, 704–714.
- [10] C. B. Kimmel, W. W. Ballard, S. R. Kimmel, B. Ullmann, T. F. Schilling, *Dev. Dyn.* 1995, **203**, 253–310.
- [11] E. Lippert, IUPAC Symposium on Hydrogen Bonding, IUPAC: Ljubljana, Yugoslavia, 1957.
- [12] W. E. Jr. Acree, D. C. Wilkins, S.A. Tucker, J. M. Griffin, J. R. Powell, *J. Phys. Chem.* 1994, **98**, 2537–2544.
- [13] R. Królicki, W. Jarzęba, M. Mostafavi, I. Lampre, *J. Phys. Chem. A*, 2002, **106**, 1708–1713.
- [14] P. Song, X. Chen, Y. Xiang, L. Huang, Z. Zhou, R. Wei, A. Tong, *J. Mater. Chem.* 2011, **21**, 13470–13475.